



Contents lists available at ScienceDirect

# Rangeland Ecology & Management

journal homepage: <http://www.elsevier.com/locate/rama>

## Estimating Forage Utilization with Drone-Based Photogrammetric Point Clouds☆☆☆



Jeffrey K. Gillan <sup>a,\*</sup>, Mitchel P. McClaran <sup>a</sup>, Tyson L. Swetnam <sup>b</sup>, Philip Heilman <sup>c</sup>

<sup>a</sup> University of Arizona, School of Natural Resources & Environment, Tucson, AZ 85721, USA

<sup>b</sup> University of Arizona, BIO5 Institute, Tucson, AZ 85721, USA

<sup>c</sup> USDA Agricultural Research Service, Southwest Watershed Research Center, Tucson, AZ 85719, USA

### ARTICLE INFO

#### Article history:

Received 19 September 2018

Received in revised form 4 February 2019

Accepted 27 February 2019

#### Key Words:

drone  
remote sensing  
structure-from-motion photogrammetry  
rangelands  
UAS

### ABSTRACT

Monitoring of forage utilization typically occurs at sample locations, or key areas, selected for their presumed potential to represent utilization across pastures. However, utilization can vary greatly across landscapes and may not be well represented by traditional ground-based sampling without great effort. Remote sensing from satellite and manned airborne platforms offers spatial coverage at landscape scale, but their poor spatial resolution (satellite) and cost (manned airborne) may limit their use in monitoring forage utilization. High-resolution photogrammetric point clouds obtained from small unmanned aerial systems (sUAS) represent an appealing alternative. We developed a method to estimate utilization by observing the height reduction of herbaceous plants represented by 3-dimensional point clouds. We tested our method in a semiarid savanna in southern Arizona by comparing utilization estimates with ground-based methods after a month-long grazing duration. In six plots, we found strong correlation between imagery and ground-based estimates ( $r^2 = 0.78$ ) and similar average estimate of utilization of across all plots (ground-based = 18%, imagery = 20%). With a few workflow and technological improvements, we think it is feasible to estimate point cloud utilization over the entire pasture (150 ha) and potentially even larger areas. These improvements include optimizing the number of images collected and used, equipping drones with more accurate global navigation satellite systems (e.g., Global Positioning System), and processing images with cloud-based parallel processing. We show proof of concept to provide confident estimates of forage utilization patterns over large pastures and landscapes, at levels of spatial precision that are consistent with ground-based methods. The adoption of drone-based monitoring of utilization of forage on rangelands could follow the paradigm shift already demonstrated by Global Positioning Systems and Geographic information systems technologies, where the initial high computing costs were reduced, use became the norm, and the availability of more precise spatial patterns was applied to prescribe and evaluate management practices.

© 2019 The Society for Range Management. Published by Elsevier Inc. All rights reserved.

### Introduction

Forage utilization, defined as the proportion of current year's production by weight consumed or destroyed by animals (Heady, 1949), can indicate levels of use and potential impacts from grazing. Managers often establish maximum levels of utilization to ensure sustainability

of use and establish monitoring protocols to detect those levels of utilization (USDI Bureau of Land Management, 1997; Smith et al., 2016). Monitoring of grazing pasture and rangelands, however, is time consuming and therefore the area sampled is limited by the availability of time and resources.

Monitoring typically occurs at a handful of sample locations, or key areas, selected for their presumed potential to represent utilization across larger pasture and landscape-scale management units. However, utilization can vary greatly across a pasture due to livestock preference for specific forage species, terrain barriers, sun exposure, and distance to water (Bailey et al., 1996). As a result, patchy distribution of utilization may not be well represented by traditional ground-based sampling, and therefore levels of utilization could be poorly represented across the large landscapes typical of western rangelands (Veblen et al., 2014). Finding more efficient methods of collecting monitoring data at pasture and landscape scales should help improve understanding of conditions and their response to management across the vast

☆ This work was supported by the USDA Agricultural Research Service and University of Arizona Agriculture Experiment Station. T.L. Swetnam was supported by NSF Grant No. DBI-1265383, DBI-1743442. Mention of a proprietary product does not constitute a guarantee or warranty of the products by the US government or the authors and does not imply its approval to the exclusion of other products that may be suitable.

☆☆ Original UAS imagery and GNSS-RTK ground control points are hosted in CyVerse DataCommons <https://doi.org/10.25739/Gayd-6j02>.

\* Correspondence: Jeffrey K. Gillan, School of Natural Resources & Environment, 1064 E Lowell St, Tucson, AZ 85721, USA.

E-mail address: [jgillan@email.arizona.edu](mailto:jgillan@email.arizona.edu) (J.K. Gillan).

rangelands in the western United States and world (Booth and Tueller, 2003).

Remote sensing from satellite and manned airborne platforms offers spatial coverage at landscape scale (Booth and Cox, 2011), but their poor spatial resolution (satellite) and cost (manned airborne) may limit their use in monitoring forage utilization. High-resolution imagery from small unmanned aerial systems (sUAS), commonly known as drones, represents an alternative (Rango et al., 2009; Anderson and Gaston, 2013). The availability of low-cost sensor-carrying sUAS and the advancement of photogrammetric software has made on-demand 3-dimensional (3D) depictions of rangeland vegetation relatively easy to produce. Further, sUAS have the potential for frequent on-demand deployments yielding imagery at scales sufficiently fine to resolve low-stature herbaceous vegetation. Though sUAS imagery cannot be expected to cover the large geographic extents available from satellites or manned aircraft, they can easily exceed the extent of area covered by most ground-based campaigns. These new tools and the imagery products we can create with them have the potential to address a number of management concerns regarding forage use by livestock and wildlife, quality of wildlife habitat, and amount of wildfire fuels.

There has been little research using remote sensing to measure forage utilization from any platform or scale. The only known study to explicitly estimate utilization did so by relating simulated browse (manually removed winterfat leaves to simulate livestock browsing) with UAS imagery spectra (Quilter and Anderson, 2001). There is, however, a large and growing body of literature on remotely sensing forage biomass where one could presumably estimate utilization with biomass measures at two points in time. The most common method relies on the relationship between ground-based measures of biomass with coregistered imagery spectra. This method has been demonstrated with satellite imagery (Todd et al., 1998; Kawamura et al., 2005; Marssett et al., 2006; Edirisinghe et al., 2011; Feng and Zhao, 2011; Schucknecht et al., 2017), manned airborne imagery (Beeri et al., 2007), and sUAS imagery (Wang et al., 2014). However, seasonal and phenological changes in spectra may limit the general application of this approach given the need for multitemporal estimates of biomass.

Alternatively, 3D representation of vegetation can estimate biomass and should be robust across the seasons when spectra is likely to change. Cunliffe et al. (2016), for example, estimated biomass of grass (*Bouteloua eriopoda*) with grass volume derived from UAS-obtained photogrammetric point clouds. While this method overcomes the limitation of relating spectral properties to biomass, it has a new challenge of accurately measuring herbaceous vegetation height. This is usually achieved by subtracting a digital terrain model (DTM) from a digital surface model (DSM). However, using a photogrammetric approach to make a DTM is challenging because it cannot “see” underneath dense vegetation and thus the ground elevation under grasses must be interpolated from nearby ground elevations (Swetnam et al., 2018). In a natural rangeland environment, unbroken extents of vegetation and/or sloped terrain can lead to incorrect estimation of ground elevations under vegetation. These challenges often introduce vertical errors in canopy height models, which can make a big difference in the volume and biomass estimates of low stature vegetation such as forage grasses. Studies in crop fields have produced accurate DTMs when the vegetation is not present (Bendig et al., 2014). This strategy does not work in many rangeland environments where perennial grasses (albeit dormant) are present year-round.

We report a “proof of concept” assessment of a remotely acquired photogrammetric method for estimating utilization without having to estimate biomass. Forage utilization in rangeland settings can be determined from the proportion of plants whose height has been reduced by grazing (Roach, 1950). We can mimic this method by measuring change in plant height using point cloud analysis. We evaluated this method in a mixed shrub-grass savanna by comparing ground-based estimates and sUAS point cloud estimates of forage utilization following a month-long grazing event. This is the first

study to use remotely sensed data to directly estimate forage utilization by grazing cattle.

The objectives for this study were to 1) estimate forage utilization by differencing pregrazed and postgrazed sUAS photogrammetric point clouds, 2) compare imagery-derived utilization with ground measurements of utilization at transect and plot scales, and 3) identify critical improvements that will extend this method to cover pasture-sized areas.

## Methods

### Study Area

The experimental area (pasture UA-C) is a 147-ha fenced pasture on the Santa Rita Experimental Range (SRER) in southern Arizona (31°48'36"N, 110°50'51"W, elevation 1 174 m; Fig. 1; <http://cals.arizona.edu/srer>). SRER soils are characterized as clay loams, sandy loams, and limey upland soils. This semiarid area experiences a typical Sonoran Desert bimodal pattern of precipitation where most moisture falls in late summer and the rest is primarily in December and January (McClaran and Wei, 2014). Mean annual temperature and precipitation are 19°C and 35.8 cm yr<sup>-1</sup>, respectively. The pasture lies on a sandy loam upland ecological site within Sonoran Desert grassland savanna (MLRA 41-3). The dominant herbaceous forage species included *Eragrostis lehmanniana* (Lehmann lovegrass), *Digitaria californica* (Arizona cottontop), *Muhlenbergia porteri*. (bush muhly), and *Aristida* ssp. (threeawn). Woody species consisted of *Prosopis velutina* (mesquite), *Gutierrezia sarothrae* (broom snakeweed), *Zinnia pumila*, *Opuntia* ssp. (prickly pear), and *Cylindropuntia* ssp. (cholla).

In calendar yr 2016, there was 39.5 cm of precipitation in the study pasture, 77% of which fell in July, August, and September. Herbaceous grass production follows the late summer monsoon rain. At peak greenness (mean Landsat 8 NDVI = 0.45) as a proxy for peak forage production, 80 animal units consisting of cow/calf pairs entered the pasture on 22 August, 2016 and remained until 23 September, 2016. At the time of withdrawal, herbaceous vegetation had already begun senescence indicated by lower NDVI values (mean = 0.36) and a lighter green color. This timing near the end of the growing season minimized the amount of regrowth following defoliation compared with timing earlier in the growing season.

### Ground Methods

Within the study pasture, we chose six randomly placed points to compare ground-based and sUAS imagery estimates of utilization (see Fig. 1). From the random points, we chose a random azimuth to orient the rectangular plot. The baseline of the plots was oriented at 220° azimuth from the plot point. Perpendicular from the baseline, we established 5 sampling transects, each 30 m long. Transects were spaced approximately 20 m apart, but that distance varied depending on the ability to navigate through or around mesquite and cactus. The plot size was ~0.27 ha or 100 × 30 m.

Following the removal of cattle from the pasture, we measured utilization using the “ungrazed plant” method along each transect. The method (Roach, 1950) was developed at the SRER and is based on the grazing habits of cattle. With ample available forage, cattle are likely to graze a grass clump once and move on to the next. Because of this behavior, there is a relationship between the percentage of ungrazed clumps and utilization of forage. At every other pace along the transect (20 total observations), the observer recorded the nearest herbaceous plant as “grazed” or “ungrazed.” Classifying lightly grazed plants as “grazed” is likely to overestimate forage use because the tops of grass plants generally contain a small proportion of the plants' biomass. To identify these lightly grazed plants, we employed the grazed class method (Schmutz et al., 1963), which consists of species-specific photo guides for estimating biomass use. Plants with ≤ 10% use were

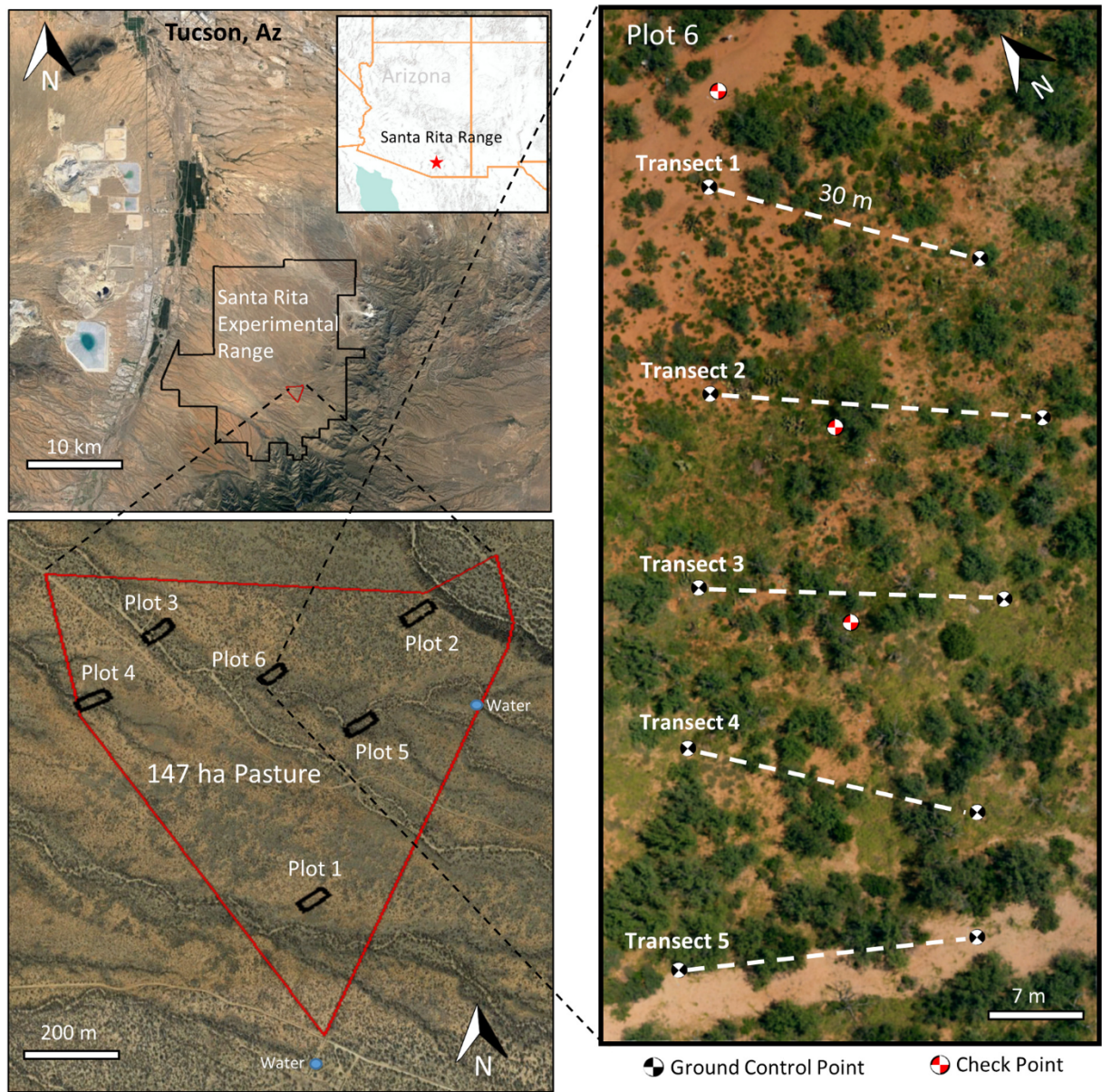


Figure 1. Study area and plot design on the Santa Rita Experimental Range in southern Arizona.

classified as “ungrazed.” The percent of ungrazed observations was entered as  $x$  in the linear formula.

$$\%utilization = 79.9451 - 0.8705x \tag{1}$$

Utilization was calculated for each transect and for each plot (aggregate of five transects).

In addition, we estimated utilization with before- and after-grazing measures of forage biomass, a method that is commonly used in other rangeland systems. Immediately before and immediately after the grazing period, we estimated forage production along each transect using the comparative yield method (USDI Bureau of Land Management, 1999). For each plot, forage was clipped, dried, and weighed from three calibration frames ( $40 \times 40$  cm) representing low, medium, and high amounts of forage. These frames were given scores of 1, 3, and 5, respectively. These calibration frames are used to train the observer to visually interpret all additional frames with a score of 0–5. This method allowed for quicker data collection and the ability to cover a larger area than destructive sampling methods. We estimated forage

production in 20 frames along each transect for a total of 100 frames per plot. From the forage production data, we calculated utilization as:

$$\%utilization = 1 - \left( \frac{biomass_{post-grazed}}{biomass_{pre-grazed}} \right) \tag{2}$$

where utilization is calculated from the ratio of biomass measured pregrazed to postgrazed. We refer to this as the “biomass change” method hereafter. We calculated utilization with the biomass change method at only the plots (aggregate of five transects) because we did not record pregrazed estimates for each transect.

#### Image Acquisition

Immediately before and after cattle grazing, we acquired high-resolution drone imagery of each plot with DJI Phantom 3 Professional and Phantom 4 multirotor drones (Table 1 for image acquisition specifications). These drones weigh ~3 lbs, have electric motors, and typically

**Table 1**  
Image acquisition specifications.

Aircraft	DJI Phantom 3 Professional & Phantom 4 multirotors
Sensor	12 mpix; 33 msec rolling shutter readout; RGB
Image format	jpeg file format; 5.2 MB per image; bit depth R(8) + G(8) + B(8)
Autopilot	Altizure v 3.0 for Ipad
Flying height	~20 m above ground level
Image dimensions	8–10 mm ground sampling; 31 × 23 m footprints
Ground speed	4–5 m/sec
Image count per plot	~950 total; 190 nadir, 760 42° oblique (190 N, 190 S, 190 W, 190 E)
Image forward and side overlap	75–80%
Flying time per plot	45 min

have 20-min flight endurance. The Phantom series are the most ubiquitous drones on the market and are off-the-shelf ready to fly with modest price points around \$1 500. We acquired the imagery for each plot using autonomous grid pattern missions programmed in Ipad application Altizure v 3.0 (<https://next.altizure.com>). We flew low to the ground (20 m above ground level) in order to get high-resolution imagery (8–10 mm) capable of resolving low-stature herbaceous plants. In the structure-from-motion (SfM) photogrammetry approach we employed, a high number of overlapping images is recommended to reconstruct complex features (Westoby et al., 2012; Smith et al., 2015). However, the optimized number of images needed to reconstruct perennial dryland grasses was unknown before this study. Consequently, we blanketed each plot with 900–1 000 images with high overlap (80%), likely more imagery than what is necessary for reconstruction. We acquired imagery at nadir and 42-degree oblique angles because the inclusion of oblique images in the sparse point cloud step has been shown to improve scene geometry compared with only nadir images (James and Robson, 2014). It was hypothesized that oblique images might also improve reconstruction of herbaceous vegetation at the base of mesquite trees, areas that are less visible from nadir-only imagery. Each plot took approximately 45 minutes to fly, including two battery changes. Wind speed during the flights typically ranged from 5 to 10 mph, not strong enough to disrupt operations.

Because the expected positional accuracy of the drone global navigation satellite system (GNSS) is poor (1–2 m horizontally and 5–10 m vertically from true location), we surveyed ground control points (GCPs) to be used in the photogrammetry processing. On each plot, we surveyed 13 GCPs. Ten were used in the photogrammetry processing, and three were held back as x, y, and z check points. The GCPs were located on the ends of each vegetation transect (see Fig. 1). Each GCP consisted of a 17-cm diameter round plastic lid mounted on a 0.5-m rebar stake. The lids were painted black and white in an iron cross pattern. We experimented with but ultimately abandoned the use of coded targets, patterns that can be detected automatically by software, because it could not reliably locate GCPs in oblique imagery. We surveyed the GCPs with a Trimble R10 real-time kinematic GNSS, a setup consisting of a base station and rover. Points were surveyed in NAD 83 UTM Zone 12 N projection with a horizontal precision of 5–7 mm and vertical precision of 6–16 mm.

#### Point Cloud Generation

We used image-based 3D reconstruction software Agisoft Photoscan v 1.3 (<http://www.agisoft.ru>) for point cloud generation. Each point in the cloud is an x, y, z location of a surface feature with its natural color assigned to it. The SfM process of making point clouds is well documented (Snavely et al., 2008; Westoby et al., 2012; Smith et al., 2015; Eltner et al., 2015), so it will be abbreviated here. All image processing was carried out on a Windows machine with two Intel Xeon CPUs (2.4 GHz; 16 logical processors each), two EVGA GeForce GTX 1080 video cards, and 256 GB RAM.

We did “high-quality” initial alignment using the GNSS and time stamp metadata of each image to expedite the process. During this process, camera physical dimensions and lens distortion parameters were calculated with self-calibration. The pose of each exposure station was determined, and a sparse point cloud was generated. Any images that did not align or were misaligned were realigned.

After initial alignment, we located all 10 GCPs and 3 check points and marked them in the images. By locating a GCP on two overlapping images, the software estimated the locations of the GCP on all other overlapping images. We went through every image and adjusted the estimated location of the GCPs to the center of the targets. Each GCP was visible on 100–400 images. Points in the center of the plot generally had more image projections, and vegetation blocked the view of the GCP in some images. Manually adjusting GCPs locations was the most time-consuming aspect of the point cloud generation.

We used the GCPs for a bundle adjustment optimization procedure. Following the recommendation of James et al. (2017a), we optimized parameters focal length (f), principal point coordinates (cx, cy), radial distortion (k1, k2), and tangential distortion (p1, p2). We also optimized to correct for rolling shutter effect present in Phantom sensors (Vautherin, 2016). Next, we used the “gradual selection” tool to identify and remove low-quality sparse points with the following criteria: reprojection error > 0.5 pixels, reconstruction uncertainty > 30, and projection error > 3. The sparse cloud was optimized (bundle adjustment) after each removal of low-quality points.

We created dense point clouds using an ultra-high-density setting, which attempts to create a point for every image pixel, a desirable behavior for fine-scale vegetation. For this step, we sought to optimize the number of images needed to reconstruct grass with high detail while limiting processing time. On one plot we experimented with the number of images used in dense reconstruction testing a model using only nadir images (150–200) and a model using nadir + all oblique images (900–1 000) for dense reconstruction. The nadir only dense point cloud had ~27 million points and took approximately 5–6 h to process. Comparatively, the nadir + oblique point cloud had ~87 million points and took upwards of a week to process. However, higher point density does not necessarily indicate better or more detailed grass height reconstruction. We tested grass height difference of the two point clouds by subtracting one from the other using M3C2 tool in CloudCompare. A detailed description of these methods is in the “Point Cloud Filtering” and “Point Cloud Differencing” sections of this paper. The nadir only point cloud was on average only 1 cm lower in height than the nadir + oblique point cloud, which suggests nadir only imagery is a more efficient approach.

Another concern of eliminating oblique images was losing the ability to detect and model herbaceous vegetation under mesquite trees. We evaluated this concern on one plot and found herbaceous vegetation to be visible and reconstructed at the base of nearly all mesquites. We are, however, giving up some ability to model grass at the base of some mature mesquite trees that have wide obscuring canopies. These were rare occurrences in our study plots that we assume should not significantly alter utilization estimates. We proceeded to carry out dense point cloud reconstruction for all the plots using nadir images only (Fig. 2A). The plot point clouds typically had between 25 and 50 million points with density ranging from 3 000 to 5 000 points·m<sup>-2</sup>.

#### Point Cloud Filtering

The goal of filtering is to remove any points that are not of interest in the analysis. For this study, we were interested in only herbaceous vegetation. Using the “classify points” tool in Photoscan, we identified and removed points representing tall woody trees and shrubs while retaining low-stature vegetation such as grasses and forbs (Fig. 2B). Cunliffe et al. (2016) and Gillan et al. (2017) both demonstrated the use of this type of filtering approach in semiarid shrublands in New Mexico. This point filtering tool is a type of maximum local slope

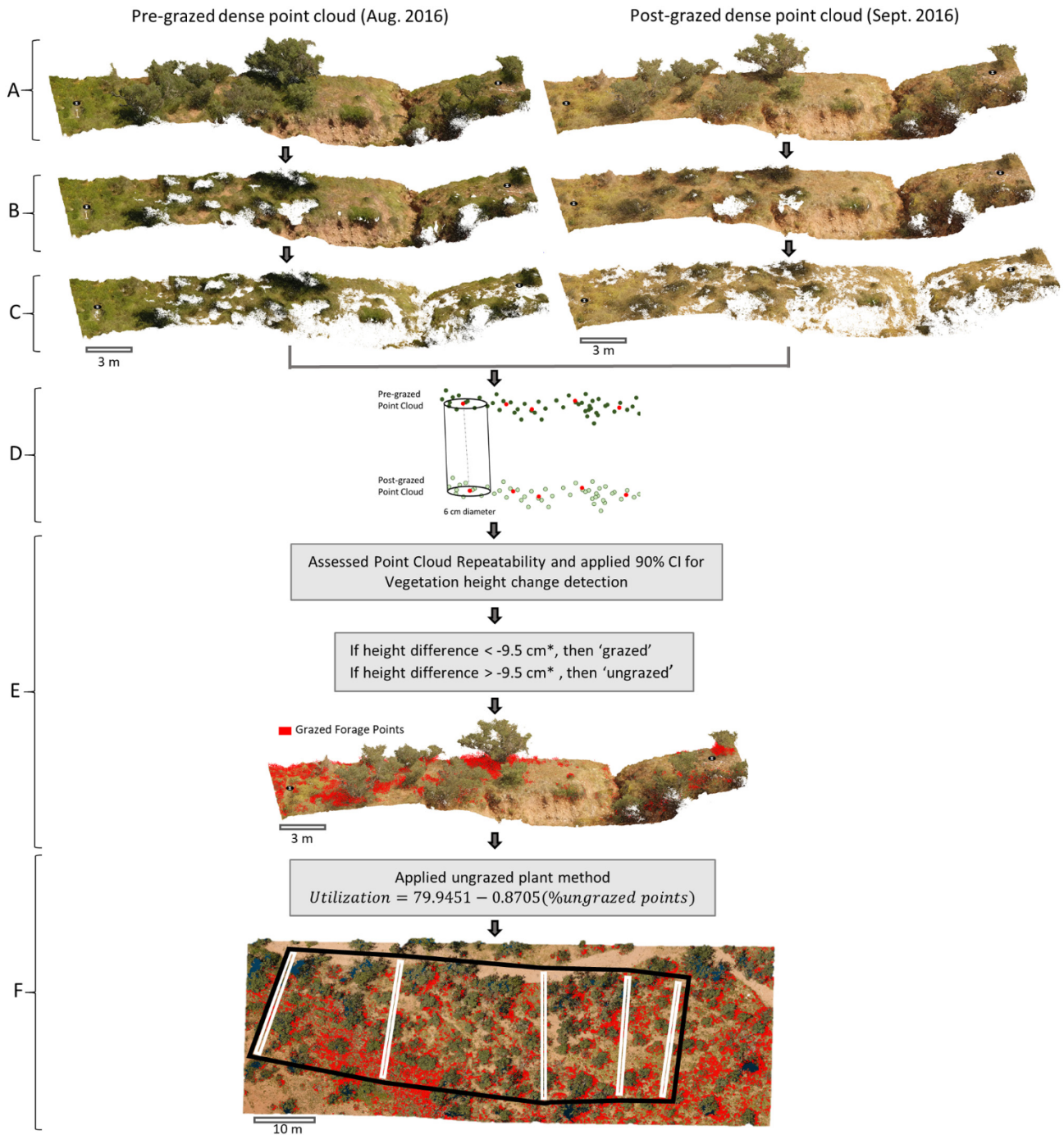


**Figure 2.** Workflow to calculate forage utilization with point clouds. **A**, We created a drone-based structure-from-motion photogrammetry point clouds before and after a month-long grazing event. Here we depict a single 30-m transect. **B**, Tall woody vegetation was removed using a local maximum slope threshold in Agisoft Photoscan. **C**, Bare ground and woody stems were filtered with a green leaf algorithm, leaving only herbaceous vegetation. **D**, Vertical height change estimated by subtracting pregrazed herbaceous points from postgrazed herbaceous points using M3C2 in CloudCompare. **E**, Repeatability of height change estimated at each plot and applied a 90% confidence interval to set a vegetation height change detection threshold (\*threshold varies per plot). Each point was labeled as “grazed” or “ungrazed” on the basis of this threshold. **F**, The percentage of ungrazed points was entered into the ungrazed plant method equation (Eq. (1)) to estimate utilization. We compared point cloud utilization with ground-based utilization at individual transects (white rectangles), plot aggregated from five transects, and the entire plot (black rectangle).

filter (Montealegre et al., 2015) where the lowest elevation point within a user-defined grid cell is assumed to be ground. All additional ground points are identified on the basis of a user-defined maximum angle and distance from the origin ground point. To identify and remove woody trees and shrubs, we found the best combination of parameter values were a grid size of 2 m, a maximum angle of 18 degrees, and a maximum distance of 0.5 m. However, no filter is perfect, so some tree stems and small shrubs were likely to remain. We exported the point

clouds in log ASCII format (las) format, in projection NAD 83 UTM Zone 12 N.

In the open-source program CloudCompare (Girardeau-Montaut, 2011), we further filtered the point clouds to remove nonherbaceous vegetation points (i.e., bare ground, rocks, woody vegetation stems) with a color threshold (Fig. 2C). We calculated a green leaf algorithm ( $\frac{G*2-R-B}{G*2+R+B}$ ; Louhaichi et al., 2001) on the colored points and applied a simple threshold to separate the herbaceous vegetation from all other

surface features. We found that a green leaf algorithm value  $> 0.035$  was an appropriate threshold for identifying vegetation points. This cutoff value varied slightly between plots due to nuanced soil and vegetation color, as well as illumination differences. We removed the nonherbaceous points, leaving point clouds consisting of only herbaceous vegetation before and after grazing.

### Point Cloud Differencing

We used the Multiscale Model to Model Cloud Comparison (M3C2) point cloud differencing tool (Lague et al., 2013; James et al., 2017b) in CloudCompare to subtract pregrazed herbaceous points from postgrazed herbaceous points in the vertical (z) plane only. This type of analysis is similar to the well-established method of digital elevation model differencing (Brasington et al., 2003; Wheaton et al., 2009) but uses points instead of gridded raster surfaces. Doing the analysis with points removes the step of having to interpolate the points into an elevation surface. Before differencing, we thinned and smoothed the pregrazed and postgrazed point clouds to reduce noise and absorb horizontal coregistration error (Table 2). M3C2 calls this subset of points “core points.” We applied a 6-cm horizontal distance between core points, effectively removing 96% of the total points within a cloud, resulting in 120–200 core points  $\cdot \text{m}^{-2}$ . The elevation values of the core points were calculated as an average of all points within a 3-cm spherical radius of the core point. In the vertical (z) plane only, the algorithm measures the distance from the averaged core point in the pregrazed cloud to the average core point in the postgrazed cloud (Fig. 2D). If there are not core points from both clouds in the same vertical cylinder, then no differencing occurs.

We performed point cloud differencing for each transect and for entire plots (minimum convex polygon surrounding the five transects). We isolated each transect in CloudCompare using the “cross-section” tool. We set the width of the transects at 1 m, an area we thought would contain the 40-cm wide frame measurements with some additional space for possible spatial registration errors. We then exported the M3C2 point data to .csv format. We deleted any point difference values  $< -1.0$  m or  $> 1.0$  m because grass could not have been grazed or grown a meter in the 1-mo duration of the study. The sporadic existence of such erroneous values is due to some kind of error, most likely an unfiltered tree or shrub point differenced from underlying grass points. For each plot, the existence of these points was typically  $< 0.5\%$ .

### Repeatability Error and Threshold for Detecting Vegetation Height Change

Because we estimated vertical differences between point clouds at two points in time, it was essential to quantify the repeatability (precision) error of point cloud reconstructions in order to separate true grass height change from measurement error. Good point cloud reconstruction requires finding the same surface features in multiple images. This can be an easier task for solid features (e.g., bare-ground, rocks) that are visible from several angles. For vegetative surfaces, even slight differences in image perspectives or illumination can cause features to be obscured or have altered texture between successive images. This phenomenon can cause point cloud reconstructions of vegetation to

be less repeatable. For each plot we measured the repeatability between the before- and after-grazing point clouds by looking initially at the check points. With perfect repeatability, the check point modeled coordinates should not change between two points in time. The observed change can be used to estimate repeatability error primarily due to scene geometry, lens calibrations, or reference quality. In addition to the checkpoint analysis, we developed a herbaceous vegetation reconstruction error term. We did so by reconstructing a 3D scene twice using two independent image sets acquired within 30 min of each other (plot 5 on 6 September, 2016). We used M3C2 to vertically differentiate the point clouds (same methods described previously). In theory, there should be no vertical difference between the point clouds, so any difference is due to reconstruction error. The standard deviation of checkpoint differences was 3.0 cm. As expected, the standard deviation of herbaceous points (using same filtering methods) was larger at 7.7 cm. We calculated the total repeatability error for each plot as the standard deviation of the checkpoint vertical repeat error plus 4.7 cm (7.7 cm herbaceous height standard deviation [SD] minus 3.0 checkpoint SD) for herbaceous reconstruction error (Fig. 2E; see Table 2). On the basis of this two-part error assessment, the vegetation vertical repeatability error among plots ranged from 5.2 to 7.5 cm (see Table 2).

We added a 90% confidence interval to the repeatability error to set a grass height change detection threshold that reduces type I errors (false positive for grazing designations).

$$\text{Grass height change detection threshold} = (\text{checkpoint SD} + 4.7 \text{ cm}) \cdot 1.645 \quad (3)$$

Using plot 5 as an example, the repeatability SD of the checkpoints was 1.1 cm. We added the grass reconstruction error of 4.7 cm for a total of 5.8 cm. The  $Cl_{90} = 5.8 \cdot 1.645 = 9.5$  cm. Using this logic, grass height must be reduced by 9.5 cm in this plot for it to be considered grazed. Vegetation height change detection thresholds ranged from 8.5 to 12.3 cm (see Table 2).

We applied the vegetation height change detection threshold to all core points in the differenced point clouds and labeled each point as grazed or ungrazed (Fig. 2E). We then calculated the percentage of ungrazed core points within the total forage core points and used that value in the “ungrazed plant” method equation (see Eq. (1); Fig. 2F) to estimate forage utilization. We then compared these values of utilization with ground-based estimates of utilization at transect scale, plot scale aggregated from five transects and plot scale with all measurements within a polygon surrounding the transects (Fig. 2F). Transect 5 of plot 4 was omitted from the study because we failed to image the entire plot during August acquisition. Our comparative analysis contained 29 transects within 6 plots.

### Accuracy of Point Cloud Maximum Plant Heights

Accuracy in this case refers to how well we can create a point cloud to capture the “true” vegetation heights. This differs from the previous section that was primarily concerned with the repeatability of point cloud generation. Knowing how well point cloud reconstructions represented the true structure of the grass indicates how sensitive our

**Table 2**  
Check point ( $n = 3$  per plot) repeatability and vegetation height change detection threshold

Plot	Check point x repeatability RMSE (cm)	Check point y repeatability RMSE (cm)	Check point z repeatability RMSE (cm)	Check point z repeatability SD (cm)	Grass repeatability error SD (cm)	Total repeatability error SD (cm)	$Cl_{90}$ height change threshold (cm)
1	2.0	1.8	1.7	1.2	4.7	5.9	9.7
2	0.8	1.1	0.8	1.0	4.7	5.7	9.3
3	0.8	1.5	1.9	0.5	4.7	5.2	8.5
4	2.5	1.4	2.3	2.8	4.7	7.5	12.3
5	0.8	1.1	0.9	1.1	4.7	5.8	9.5
6	0.7	0.6	0.9	1.0	4.7	5.7	9.3

methods are to detecting a change in height. It may also provide an explanation for differences between the ground and point cloud methods for estimating utilization. Before this study, the accuracy of photogrammetrically reconstructing herbaceous vegetation from UAS imagery was unknown in our study ecosystem. To quantify vegetation maximum height accuracy, we used a hand-held tape to measure the maximum height of 21 herbaceous plants (grasses and forbs) immediately before the August image acquisition. We then compared the ground-based measured heights with the point cloud heights of those same 21 plants using CloudCompare.

**Results**

*Agreement Between Imagery and Ground-Based Ungrazed Plant Method of Estimating Utilization*

At the transect scale, there was a poor linear relationship between point cloud and “ungrazed plant” methods of utilization ( $R^2 = 0.011$ ; Fig. 3A), and differences ranged from an overestimation (below 1:1 line) of 38% to an underestimation (above 1:1 line) of 34% of ground-based value. The median absolute difference between the methods was 13% (Fig. 3D). At the aggregated transect scale, the agreement between the point cloud and ungrazed plant method was much stronger than the transect scale ( $R^2 = 0.78$ ; Fig. 3B). Method differences ranged from an overestimation of 8% to an underestimation of 6% and median absolute difference was 5.2% (Fig. 3D). Agreement at the plot scale was also strong ( $R^2 = 0.81$ ; Fig. 3B) and ranged from an overestimation of 8% to an underestimation of 3%, and the median absolute difference was 6% (Fig. 3D). Interestingly, at both

**Table 3**

Utilization estimated with ground-based methods and point cloud differencing methods arranged from most to least utilization by plot. Normal approximation used to generate standard error and 95% confidence interval.

Forage utilization	Ungrazed plant aggregated transects	Biomass change aggregated transects	Point cloud differencing aggregate transects	Point cloud differencing plot scale
Most	Plot 6 (24.2%)	Plot 3 (37.5%)	Plot 6 (32.0%)	Plot 6 (31.1%)
	Plot 3 (22.4%)	Plot 4 (23.4%)	Plot 3 (26.8%)	Plot 3 (28.5%)
	Plot 5 (20.7%)	Plot 5 (21.8%)	Plot 4 (25.1%)	Plot 5 (26.8%)
	Plot 4 (16.4%)	Plot 6 (22.2%)	Plot 5 (23.3%)	Plot 4 (25.1%)
	Plot 2 (14.6%)	Plot 1 (13.9%)	Plot 1 (9.4%)	Plot 1 (13.7%)
	Plot 1 (12.9%)	Plot 2 (13.5%)	Plot 2 (8.5%)	Plot 2 (11.1%)
Average	18.5 ± 4.7%	23.3 ± 9.1%	20.8% ± 10.1%	22.7% ± 8.6%

the aggregated transect and entire plot scales, the ground-based estimate of utilization was underestimated when the point cloud estimate was < 15% utilization and overestimated when > 15% (Fig. 3B).

The average utilization of all six plots combined was estimated at 18.5% using the ungrazed plant method (Table 3). The point cloud method with five aggregated transects had utilization of 20.8%, while the entire plot point cloud method estimated a total utilization of 22.8% for all six plots. In terms of plot rank order (most to least), the point cloud methods were similar to the ungrazed plant method with some slightly different ordering (see Table 3). The discrepancy in rank order between the ground-based and point cloud methods was the result of only a few percentage points.

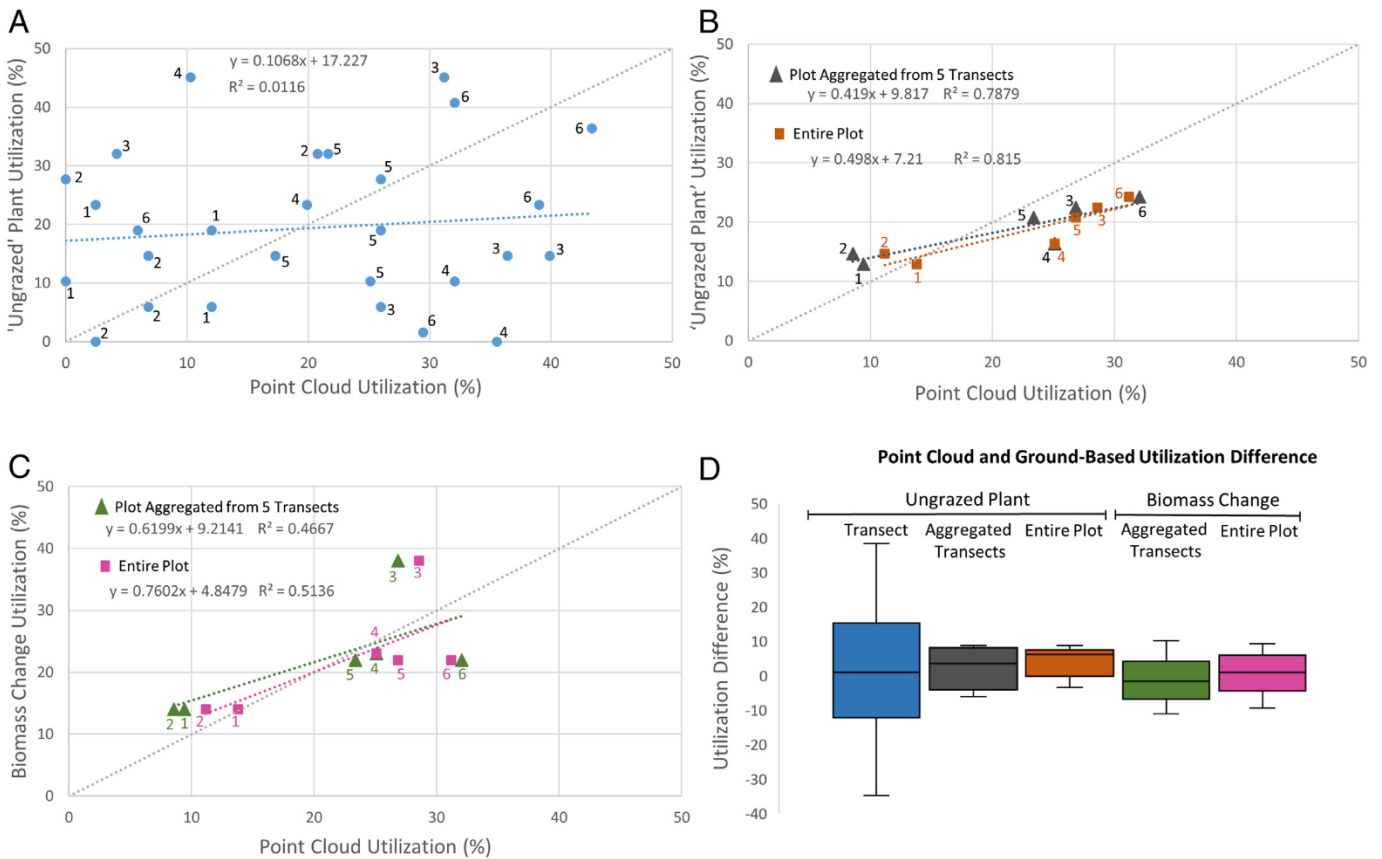


**Figure 3.** A, Linear regression between point cloud and ungrazed plant method estimates of utilization with transects as the sample unit. Plot numbers are labeled 1–6 on the graphs. B, Linear regressions between point cloud and ungrazed plant method with the sample units being plot aggregated from five transects and entire plot. C, Linear regressions between point cloud and biomass change method with the sample units being plot aggregated from five transects and entire plot. D, Box plots showing difference between point cloud and ground-based method utilization. Whiskers show the range, boxes show the interquartile range, and the middle line represents the median.

### Agreement Between Imagery and Ground-Based Biomass Change Method of Estimating Utilization

The agreement between the point cloud methods and biomass change field method was not as robust as the ungrazed plant method. At the aggregated transect scale, the agreement between the point cloud and biomass change estimates of utilization was modest ( $R^2 = 0.46$ ;  $b = 0.61$ ; Fig. 3C). Differences between the point cloud and biomass change estimates of utilization ranged from an overestimation of 9.8% to an underestimation of 10.6%, and median absolute difference was 4.7% (Fig. 3D). At the plot scale, the agreement was also modest ( $R^2 = 0.51$ ;  $b = 0.76$ ; Fig. 3C) and differences between the point cloud and biomass estimates of utilization ranged from an overestimation of 8.9% to an underestimation of 8.9%. The median absolute difference was 3.6% (Fig. 3D). As occurred with the ungrazed plant results, at both the aggregated transect and plot scales, the biomass change estimate of utilization was underestimated when the point cloud estimate was  $< 15\%$  utilization and overestimated when  $> 15\%$  (Fig. 3C).

The utilization of all six plots combined was estimated at 23.3% using the biomass change method (see Table 3). The point cloud method with five aggregated transects had utilization of 20.8%, while the entire plot point cloud method estimated a total utilization of 22.8% for all 6 plots. Utilization rank order using the biomass change method was a bit different than the other methods (see Table 3). Most notably, it estimated plot 3 to have the highest utilization (37.5%), 15% higher than the ungrazed plant method, 11% higher than the aggregated transect point cloud method, and 9% higher than the entire plot point cloud method.

### Accuracy of Point Cloud Maximum Plant Heights

On average, the point maximum plant heights were 45% of ground measured heights with SD of 12% (Fig. 4; Appendix Table A1). Underestimation of grass plant height is likely a function of imagery that is too

coarse to detect and match features in the diffuse canopy and possible movement of that canopy caused by wind.

### Discussion

Our “proof of concept” assessment provides results that support the use of photogrammetric point cloud differencing as a viable alternative to ground-based estimates of forage utilization in a semiarid mixed-shrub savanna ecosystem. There was strong agreement between utilization estimates using drone-based point cloud differencing of plant height and the ground-based ungrazed plant method (developed at SRER) for which it was expected to mimic. There was also good agreement with the biomass change ground method. This suggests that the point cloud method of detecting change in plant height could provide reliable estimates of utilization in other rangeland ecosystems and, more importantly, represent utilization over a larger spatial extent with shorter field time than the traditional ground-based estimates.

The approach of simply estimating change in plant height is advantageous compared with other remote sensing approaches that must estimate forage biomass at multiple points in time. Specifically, our method should be more stable across seasons than a 2-dimensional imagery spectra approach (e.g., Wang et al., 2014) where spectra/biomass relationships can differ among seasons for the same amount of mass. In addition, our approach should be more replicable than a 3D representation of biomass, which is reliant on making DTMs and canopy height models (e.g., Cunliffe et al., 2016). For example, our approach could be especially advantageous in ecosystems with large amounts of herbaceous cover (e.g., Great Plains) that would make it difficult to sense the ground elevation.

Agreement between ground-based and point cloud methods was stronger at plot scale than transect scale. Some of this can be attributed to the central limit theorem, which suggests that as more measurements are aggregated, the distribution will better represent the central tendency of a normal distribution leading to better agreement between

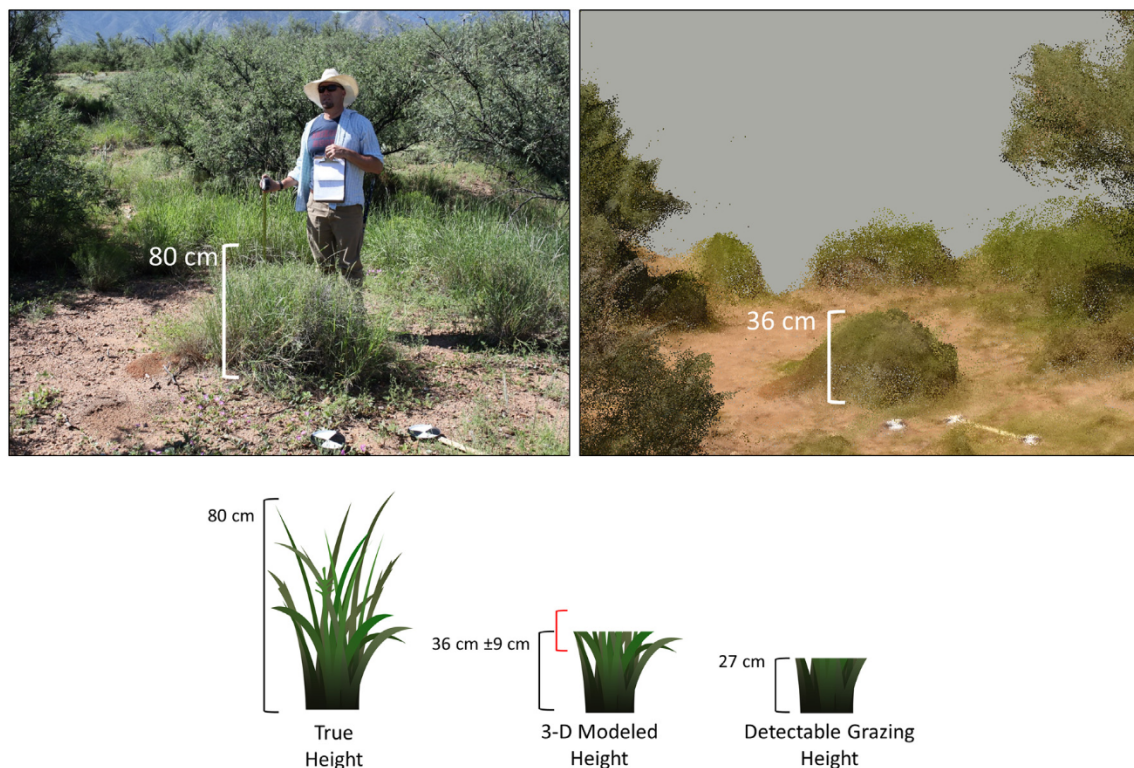


**Figure 4.** Comparing the maximum height of one Arizona cottontop (*Digitaria californica*) plant as measured in the field and estimated with sUAS-based photogrammetric point clouds. The ground-measured height was 80 cm but was modeled with point clouds to be 36 cm. Combined with point cloud repeatability error 90% confidence interval of  $\pm 9$  cm, the plant would need to be reduced to a point-cloud height of 27 cm before it could be detected as “grazed.”

the methods. In addition, the mechanics of performing the measures could contribute to the improved relationship at the plot-scale. In the ungrazed plant method, the absence of a plant at the point of observation causes the observer to seek the nearest plant, perhaps away from the transect line. This can create a mismatch in the exact ground footprint being sampled by the two methods. Also, the ground-based method is taking a sample of 20 individual plants along the transect. The point cloud method cannot distinguish individual plants and is instead taking a census of all herbaceous points in the 3-cm radius core point (~120–200 core points per m<sup>2</sup>). If there is a large plant consisting of multiple core points, some points may be classified as grazed and others as ungrazed, leading to different estimates of utilization compared with the ground-based method, which would have classified that entire plant as grazed.

Interestingly, the strong relationship between the point cloud and both the ungrazed plant and biomass change estimates of utilization occurred in spite of the point cloud representing on average 45% of grass height. We propose that the strong relationship exists because 1) grass mass is disproportionately concentrated at the lower portions of the plant (Schmutz et al., 1963; Nafus et al., 2009) and 2) we considered any plant with ≤ 10% utilization as “ungrazed” in our ground estimates. On the basis of the agreement between the field and point cloud methods, it appears that our ability to model the bottom 45% of plant height was sufficient for the level of grazing intensity in this study. For studies or management goals that require a more sensitive detection of grazing, it would be possible to reconstruct the top of grass canopies better by flying lower to the ground or using a sensor with higher spatial resolution.

We defined grazing in this study as a modeled grass height reduction with 90% confidence interval. The confidence interval can be changed to better meet management goals. Relaxing this threshold will likely increase the points that are identified as grazed, which in turn will increase utilization estimates. This could increase type I errors of identifying grass as being grazed when it was not. Consequences of this could be that the pasture is grazed less than desired. Strengthening the threshold will reduce the number of points we identified as grazed, which will lower utilization estimates. This could increase type II errors (true grazing that is not detected) for this application. Consequences of this could be that the pasture is grazed more than desired.

There are a few potential limitations of the point cloud utilization method. First, it assumes any reduction in herbaceous height past the threshold is due to grazing. Vegetation height could also be reduced by wind, rain, animal trampling, or sagging under their own weight. It may be appropriate to consider and inspect these occurrences before assuming all height reduction is due to grazing. Second, the point cloud method, along with the field methods we compared it with, are conservative estimates of utilization. It is possible that some utilization was not detected due to grass growth after being grazed. This was likely an infrequent occurrence because we timed the grazing to coincide with peak biomass. Third, it is unlikely that herbaceous species (e.g., native vs. non-native) can be distinguished with high-resolution imagery. Therefore, an estimate of *what* is being used will be challenging. Because the vegetation community was fairly simple at SRER, separating woody vegetation, herbaceous vegetation, and nonvegetation features was achievable. However, further parsing of vegetation composition will become extremely challenging when using RGB sensors.

#### *Expanding Spatial Coverage of Point Cloud Analysis*

This study demonstrated an ability to measure forage utilization at plot scales (0.25 ha). With this proof of concept established, the method must be expanded and tested over larger areas. The real advantage of drone data is to cover greater extents of land and capture more indicator variability than can be realistically sampled with ground methods.

An additional benefit of a drone approach is generating a spatial explicit map of forage utilization across a pasture. These image products will be used to better understand the response to management

practices intended to change grazing intensity and location (Brock and Owensby, 2000; Guenther et al., 2000). Utilization maps will improve our knowledge of herbivore behavior in relation to habitat characteristics such as distance from drinking water, slope, previously grazed patches, and neighboring nonforage vegetation (e.g., Bailey et al., 1996; Washington-Allen et al., 2004). A utilization map also enables a reverse assessment of the accuracy of utilization estimates based on a few ground-based estimates to represent pasture- and landscape-scale patterns. The implication is that we are able to ask how well “key areas” represent the response of utilization at the pasture-scale to changes in the management practices and growing conditions. This could be especially useful when two or more herbivore species are grazing, such as elk and cattle, and a “key area” designed for cattle may not represent the spatial use pattern of elk (Laca et al., 2010).

With a few workflow and technological improvements, we think it is feasible to estimate point cloud utilization over the entire pasture (150 ha) and potentially even larger areas. Here, we identify critical improvements to the workflow that will speed estimates of utilization measurements and increase the likelihood of adoption by practitioners.

First, we can reduce the number of images per area needed for herbaceous vegetation reconstruction. We only used the nadir images (~190 per plot) for dense point cloud generation and, therefore, could have avoided the time spent collecting and processing 760 oblique images. Woodlands or other ecosystems with more tree cover may benefit from more oblique images to view forage change at the base of the trees. The more open canopy of mesquite savanna made it possible to view herbaceous vegetation change at the base of most mesquite trees with just nadir images. Future acquisitions at SRER should consist of nadir images along with a modest amount (a few dozen) of oblique images, which have been shown to improve scene geometry in the initial alignment (James et al., 2017a). Fewer images and flight lines per area will free up our flights to cover larger areas.

Second, we should use higher-resolution sensors (more megapixels or longer focal lengths) to allow higher flight elevation and greater spatial coverage per flight time without loss of data resolution (3 000–5 000 points·m<sup>-2</sup> in our study). Higher-resolution sensors are already available for the Phantom series (Phantom 4 Pro with 20 mpx), while other studies have demonstrated the use of higher-resolution RGB cameras on other drone aircrafts (Bendig et al., 2014; Li et al., 2016; Gillan et al., 2017). We should also consider flying more than one drone at a time, which currently requires a special waiver from the US Federal Aviation Administration (CFR 107.35).

Third, we need more precise and differentially correctable GNSS on board the drones to precisely capture the coordinates of each exposure station (location of camera when image was taken) to streamline direct georeferencing and reduce reliance on ground control. The success of our point cloud differencing method depends on the point clouds being well coregistered in three dimensions. Horizontal (xy) coregistration is important in order to difference the height of same grass plant. Vertical (z) coregistration is important because it drives the vertical repeatability error and thus sets the threshold for detection of vegetation height change. We achieved good coregistration with the RTK surveyed ground control points (0.9 cm horizontal, 1.4 cm vertical). However, the survey added an entire day of field work and hours of postprocessing in Photoscan spent locating targets in the imagery.

With enough precision, direct georeferencing with RTK GNSS has the potential to greatly reduce the cost of measuring utilization over larger areas by reducing ground control requirements. Early results from drone-mounted RTK report accuracies of 2–4 cm (x, y) and 2–9 cm (z) among a variety of systems (Rehak et al., 2013; Hugenholtz et al., 2016; Forlani et al., 2018). Given that our accuracies were better than the drone-mounted RTK tests suggests that establishing permanent ground control points and RTK base stations may provide a greater return on investment for range and pastures that are routinely measured.

Alternatively, there is a little known photogrammetric technique that can be used to ensure good coregistration between multitemporal

imagery products without differential GNSS. Raw images from before and after a grazing event can actually be processed within the same project “chunk” (Korpela, 2006; Gillan et al., 2016). The initial alignment should be conducted with all images from both time periods, while the dense point clouds should be created with images from just one time period. This multitemporal approach should produce point clouds coregistered to within a few centimeters. The drawback is that the absolute georeferencing accuracy of the products will still depend on the references used (GCPs or GNSS). Also, doubling the image count in a project chunk will increase processing demands in the initial alignment.

Reducing the processing time of point clouds is the final improvement needed to expand the use of drone-based photogrammetry to estimate utilization of forage on rangelands. Measuring indicators over entire pastures will require tens of thousands of images, and processing them is a big data problem that quickly overwhelms the model of using a single powerful desktop computer. To achieve the goal of creating useable imagery products and analysis summaries in 1 or 2 days, we must shift to a cloud computing or network computing model where super computers or many regular computers tackle the problem with parallel processing nodes. Projects such as the National Science Foundation – funded Cyverse (Goff et al., 2011) and Google Earth Engine (Gorelick et al., 2017) show that big data processing is accessible now to anyone with an Internet connection, though advanced computing skills are often required. Removing the technical barriers for mass adoption will likely require a “software-as-a-service” model in which users upload images to a server and get an automated product (e.g., point cloud) in return. This shifts the burden of photogrammetry expertise, as well as purchasing and maintaining hardware. Commercial companies (e.g., DroneDeploy ([www.dronedeploy.com](http://www.dronedeploy.com)) and Agisoft ([www.agisoft.com](http://www.agisoft.com))) are offering cloud-based image product creation, but they are likely to be expensive over large extents and not specific for rangeland applications. Researchers and resource agencies should partner to develop cloud-based image processing tools specifically for estimating forage utilization and other rangeland monitoring applications.

## Implications

We focus on three implications that emerge from this successful “proof of concept” assessment showing that drone-based estimates of forage utilization can replicate estimates from traditional ground-based methods. First, there is promise to provide confident estimates of forage utilization patterns over large pastures and landscapes, at levels of spatial precision that are consistent with ground-based methods, and that promise will only increase as the technology becomes more affordable and easy to use.

The second implication is related to the clear benefit of adopting 21st century technology to assess site-specific resource conditions at exceptional precision and extent. This implies that training for rangeland managers (or at least geospatial specialists) is likely to include operation of drones for data collection and use of cloud-computing resources to handle data processing demand. Adopting these technologies may be similar to the proliferation of global positioning systems and geographic information systems in the later 20th century, where the initial high computing costs were reduced, use of the technologies became the norm, and the availability of more precise spatial patterns was applied to prescribe and evaluate management practices.

The third implication is that these technologies do not replace field skills in plant identification, knowledge of phenological patterns of growth, and ability to associate utilization patterns with the distribution of soils and geomorphic surfaces. Common sense and field setting acuity will remain critical to logical interpretation and application of the extensive and precise information available from these new technologies.

## Acknowledgments

We thank Sarah Noelle, Rachel Turner, and Kelsey Landreville for collecting vegetation ground data used in this study. We also thank

Mary Nichols of US Department of Agriculture – Agricultural Research Service for GNSS equipment and technical support.

## Appendix A

**Table A1**

Comparison of ground measured and point cloud modeled maximum height of 22 selected herbaceous plants.

Plant specimen	Species	Ground measured maximum height (cm)	Point cloud maximum height (cm)	Height proportion (point cloud height/ground-based height)
1	<i>Digitaria californica</i>	80	36	0.45
2	<i>Heteropogon contortus</i>	80	33	0.41
3	<i>Bouteloua filiformis</i>	50	30	0.6
4	<i>Eragrostis lehmanniana</i>	80	28	0.35
5	<i>Digitaria californica</i>	50	26	0.52
6	<i>Eragrostis lehmanniana</i>	100	53	0.53
7	<i>Ambrosia artemisiifolia</i>	40	13	0.32
8	<i>Aristida</i> sp.	60	10	0.16
9	<i>Kallstroemia grandiflora</i>	50	30	0.6
10	<i>Setaria leucopila</i>	58	17	0.29
11	<i>Heteropogon contortus</i>	100	44	0.44
12	<i>Digitaria californica</i>	64	40	0.62
13	<i>Eragrostis lehmanniana</i>	80	27	0.33
14	<i>Aristida</i> sp.	69	29	0.42
15	<i>Digitaria californica</i>	80	33	0.41
16	<i>Aristida</i> sp.	50	31	0.62
17	<i>Eragrostis lehmanniana</i>	75	34	0.45
18	<i>Eragrostis lehmanniana</i>	50	27	0.54
19	<i>Amaranthus</i> sp.	60	26	0.43
20	<i>Digitaria californica</i>	60	21	0.35
21	<i>Aristida</i> sp.	55	34	0.61
				Mean 0.45
				Standard deviation 0.12

**Table A2**

Point cloud marker residuals (surveyed coordinate minus modeled coordinate).

Plot	Acquisition date	Markers (n)	Residual RMSE (cm)			x, y, z
			Easting (x)	Northing (y)	Elevation (z)	
1	Aug. 2016	GCP (10)	2.6	0.5	0.7	2.8
		Check (3)	1.6	1.5	0.8	2.4
	Sept. 2016	GCP (10)	0.9	0.9	0.6	1.4
		Check (3)	1.4	1.0	2.2	2.8
2	Aug. 2016	GCP (10)	0.8	0.6	0.6	1.3
		Check (3)	1.1	1.4	2.2	2.9
	Sept. 2016	GCP (10)	0.5	0.4	0.3	0.8
		Check (3)	0.6	0.4	1.3	1.5
3	Aug. 2016	GCP (10)	1.5	1.3	0.4	2.1
		Check (3)	2.2	0.9	0.4	1.0
	Sept. 2016	GCP (10)	1.1	1.0	0.5	1.6
		Check (3)	0.8	1.6	1.6	2.4
4	Aug. 2016	GCP (10)	1.2	1.2	3.1	3.6
		Check (3)	0.6	0.6	1.5	1.7
	Sept. 2016	GCP (10)	1.4	1.7	2.1	3.1
		Check (3)	2.6	1.5	2.4	3.8
5	Aug. 2016	GCP (10)	1.0	0.6	1.0	1.6
		Check (3)	0.5	0.4	1.6	1.7
	Sept. 2016	GCP (10)	0.7	0.6	0.5	1.0
		Check (3)	0.5	0.8	0.9	1.4

Table A2 (continued)

Plot	Acquisition date	Markers (n)	Residual RMSE (cm)			x, y, z
			Easting (x)	Northing (y)	Elevation (z)	
6	Aug. 2016	GCP (10)	0.8	0.9	0.9	1.5
		Check (3)	0.9	0.5	1.8	2.0
	Sept. 2016	GCP (10)	0.9	0.5	0.7	1.3
		Check (3)	0.2	0.2	1.2	1.2
Plot average	Aug. & Sept. 2016	GCP (60)	1.1	0.8	0.9	1.8
		Check (18)	1.0	0.8	1.4	2.0

## References

- Anderson, K., Gaston, K.J., 2013. Lightweight unmanned aerial vehicles will revolutionize spatial ecology. *Frontline Ecology and the Environment* 11, 138–146.
- Bailey, D.W., Gross, J.E., Laca, E.A., Rittenhouse, L.R., Coughenour, M.B., Swift, D.M., Sims, P.L., 1996. Mechanisms that result in large herbivore grazing distribution patterns. *Journal of Range Management* 49, 386.
- Beeri, O., Phillips, R., Hendrickson, J., Frank, A.B., Kronberg, S., 2007. Estimating forage quantity and quality using aerial hyperspectral imagery for northern mixed-grass prairie. *Remote Sensing of Environment* 110, 216–225.
- Bendig, J., Bolten, A., Bennertz, S., Broscheit, J., Eichfuss, S., Bareth, G., 2014. Estimating biomass of barley using crop surface models (CSMs) derived from UAV-based RGB imaging. *Remote Sensing* 6, 10395–10412.
- Booth, D., Cox, S., 2011. Art to science: tools for greater objectivity in resource monitoring. *Rangelands* 33, 27–34.
- Booth, D., Tueller, P., 2003. Rangeland monitoring using remote sensing. *Arid Land Research and Management* 17 (4), 455–467.
- Brasington, J., Langham, J., Rumsby, B., 2003. Methodological sensitivity of morphometric estimates of coarse fluvial sediment transport. *Geomorphology* 53, 299–316.
- Brock, B.L., Owensby, C.E., 2000. Predictive models for grazing distribution: a GIS approach. *Rangelands* 53, 39–46.
- Cunliffe, A.M., Brazier, R.E., Anderson, K., 2016. Ultra-fine grain landscape-scale quantification of dryland vegetation structure with drone-acquired structure-from-motion photogrammetry. *Remote Sensing of Environment* 183, 129–143.
- Edirisinghe, A., Hill, M.J., Donald, G.E., Hyder, M., 2011. Quantitative mapping of pasture biomass using satellite imagery. *International Journal of Remote Sensing* 32, 2699–2724.
- Eltner, A., Kaiser, A., Castillo, C., Rock, G., Neugirg, F., Abellan, A., 2015. Image-based surface reconstruction in geomorphometry – merits, limits and developments of a promising tool for geoscientists. *Earth Surface Dynamics* 3, 1445–1508.
- Feng, X.M., Zhao, Y.S., 2011. Grazing intensity monitoring in northern China steppe: integrating CENTURY model and MODIS data. *Ecological Indicators* 11, 175–182.
- Forlani, G., Dall'Asta, E., Diotri, F., Cella, U.M., Roncella, R., Santise, M., 2018. Quality Assessment of DSMs Produced from UAV Flights Georeferenced with On-Board RTK Positioning. *Remote Sensing* 10, 311.
- Gillan, J.K., Karl, J.W., Barger, N.N., Elaksher, A., Duniway, M.C., 2016. Spatially Explicit Rangeland Erosion Monitoring Using High-Resolution Digital Aerial Imagery. *Rangeland Ecology & Management* 69, 95–107.
- Gillan, J., Karl, J., Elaksher, A., Duniway, M., 2017. Fine-Resolution Repeat Topographic Surveying of Dryland Landscapes Using UAS-Based Structure-from-Motion Photogrammetry: Assessing Accuracy and Precision against Traditional Ground-Based Erosion Measurements. *Remote Sensing* 9, 437.
- Girardeau-Montaut, D., 2011. CloudCompare-Open Source Project. Grenoble: OpenSource Project Available online at: <http://www.cloudcompare.org/>.
- Goff, S.A., Vaughn, M., McKay, S., Lyons, E., Stapleton, A.E., Gessler, D., Matasci, N., Wang, L., Hanlon, M., Lenards, A., Muir, A., Merchant, N., Lowry, S., Mock, S., Helmke, M., Kubach, A., Narro, M., Hopkins, N., Micklos, D., Hilgert, U., Gonzales, M., Jordan, C., Skidmore, E., Dooley, R., Cazes, J., McLay, R., Lu, Z., Pasternak, S., Koesterke, L., Piel, W.H., Grene, R., Noutsos, C., Gendler, K., Feng, X., Tang, C., Lent, M., Kim, S.-J., Kvilekval, K., Manjunath, B.S., Tannen, V., Stamatakis, A., Sanderson, M., Welch, S.M., Cranston, K.A., Soltis, P., Soltis, D., O'Meara, B., Ane, C., Brutnell, T., Kleibenstein, D.J., White, J.W., Leebens-Mack, J., Donoghue, M.J., Spalding, E.P., Vision, T.J., Myers, C.R., Lowenthal, D., Enquist, B.J., Boyle, B., Akoglu, A., Andrews, G., Ram, S., Ware, D., Stein, L., Stanzione, D., 2011. The iPlant collaborative: cyberinfrastructure for plant biology. *Frontiers in Plant Science* 2, 34.
- Gorelick, N., Hancher, M., Dixon, M., Ilyushchenko, S., Thau, D., Moore, R., 2017. Google Earth engine: planetary-scale geospatial analysis for everyone. *Remote Sensing of Environment* 202, 18–27.
- Guenther, K.S., Guenther, G.E., Redick, P.S., 2000. Expected-use GIS maps. *Rangelands* 22, 18–20.
- Hady, H.F., 1949. Methods of determining utilization of range forage. *Journal of Range Management* 2, 53–63.
- Hughenholz, C., Brown, O., Walker, J., Barchyn, T., Nesbit, P., Kucharczyk, M., Myshak, S., 2016. Spatial accuracy of UAV-derived orthoimagery and topography: comparing photogrammetric models processed with direct geo-referencing and ground control points. *Geomatica* 70, 21–30.
- James, M.R., Robson, S., 2014. Mitigating systematic error in topographic models derived from UAV and ground-based image networks. *Earth Surface Processes and Landforms* 39, 1413–1420.
- James, M.R., Robson, S., D'Oleire-Oltmanns, S., Niethammer, U., 2017a. Optimising UAV topographic surveys processed with structure-from-motion: ground control quality, quantity and bundle adjustment. *Geomorphology* 280, 51–66.
- James, M.R., Robson, S., Smith, M.W., 2017b. 3-D uncertainty-based topographic change detection with structure-from-motion photogrammetry: precision maps for ground control and directly georeferenced surveys. *Earth Surface Processes and Landforms* 42, 1769–1788.
- Kawamura, K., Akiyama, T., Yokota, H.O., Tsutsumi, M., Yasuda, T., Watanabe, O., Wang, S., 2005. Quantifying grazing intensities using geographic information systems and satellite remote sensing in the Xilingol steppe region, Inner Mongolia, China. *Agriculture, Ecosystems and Environment* 107, 83–93.
- Korpela, I., 2006. Geometrically accurate time series of archived aerial images and airborne lidar data in a forest environment. *Silva Fennica* 40, 109–126.
- Laca, E.A., Sokolow, S., Galli, J.R., Cangiano, C.A., 2010. Allometry and spatial scales of foraging in mammalian herbivores. *Ecology Letters* 13, 311–320.
- Lague, D., Brodu, N., Leroux, J., 2013. Accurate 3D comparison of complex topography with terrestrial laser scanner: application to the Rangitikei canyon (N-Z). *ISPRS Journal of Photogrammetry and Remote Sensing* 82, 10–26.
- Li, W., Niu, Z., Chen, H., Li, D., Wu, M., Zhao, W., 2016. Remote estimation of canopy height and aboveground biomass of maize using high-resolution stereo images from a low-cost unmanned aerial vehicle system. *Ecology Indicators* 67, 637–648.
- Louhaichi, M., Borman, M.M., Johnson, D.E., 2001. Spatially located platform and aerial photography for documentation of grazing impacts on wheat. *Geocarto International* 16, 65–70.
- Marsett, R.C., Qi, J., Heilman, P., Biedenbender, S.H., Watson, M.C., Amer, S., Weltz, M., Goodrich, D., Marsett, R., 2006. Remote sensing for grassland management in the arid Southwest. *Rangeland Ecology & Management* 59, 530–540.
- McClaran, M.P., Wei, H., 2014. Recent drought phase in a 73-year record at two spatial scales: Implications for livestock production on rangelands in the Southwestern United States. *Agricultural and Forest Meteorology* 197, 40–51.
- Montelegre, A.L., Lamelas, M.T., De La Riva, J., 2015. A comparison of open-source LiDAR filtering algorithms in a Mediterranean forest environment. *IEEE Journal of Selected Topics in Applied Earth Observations and Remote Sensing* 8, 4072–4085.
- Nafus, A.M., McClaran, M.P., Archer, S.R., Throop, H.L., 2009. Multispecies allometric models predict grass biomass in semidesert rangeland. *Rangeland Ecology & Management* 62, 68–72.
- Quilter, M.C., Anderson, V.J., 2001. A proposed method for determining shrub utilization using (LA/LS) imagery. *Journal of Range Management* 54, 378–381.
- Rango, A., Laliberte, A., Herrick, J.E., Winters, C., Havstad, K., Steel, C., Browning, D., 2009. Unmanned aerial vehicle-based remote sensing for rangeland assessment, monitoring, and management. *Journal of Applied Remote Sensing* 3, 033542.
- Rehak, M., Mabillard, R., Skaloud, J., 2013. A Micro-Uav with the capability of direct georeferencing. *International Archives of Photogrammetric Remote Sensing Beijing, China*. XL, pp. 4–6.
- Roach, M.E., 1950. Estimating perennial grass utilization on semidesert cattle ranges by percentage of ungrazed plants. *Journal of Range Management* 3, 182–185.
- Schmutz, E.M., Holt, G.A., Michaels, C.C., 1963. Grazed-class method of estimating forage utilization. *Journal of Range Management* 16, 54–60.
- Schucknecht, A., Meroni, M., Kayitakire, F., Boureima, A., 2017. Phenology-based biomass estimation to support rangeland management in semi-arid environments. *Remote Sensing* 9, 463.
- Smith, L., Ruyle, G., Maynard, J., Barker, S., Meyer, W., Stewart, D., Coulloudon, B., Williams, S., Dyess, J., 2016. Principles of obtaining and interpreting utilization data on rangelands. University of Arizona College of Agriculture and Life Sciences. Report AZ1375, Tucson, AZ, USA <https://extension.arizona.edu/sites/extension.arizona.edu/files/pubs/az1375-2016.pdf>, Accessed date: 30 June 2017.
- Smith, M.W., Carrivick, J.L., Quincey, D.J., 2015. Structure from motion photogrammetry in physical geography. *Progress in Physical Geography* 40, 247–275.
- Snavely, N., Seitz, S.M., Szeliski, R., 2008. Modeling the world from Internet photo collections. *International Journal of Computer Vision* 80, 189–210.
- Swetnam, T.L., Gillan, J.K., Sankey, T.T., McClaran, M.P., Nichols, M.H., Heilman, P., McVay, J., 2018. Considerations for achieving cross-platform point cloud data fusion across different dryland ecosystem structural states. *Frontiers in Plant Science* 8, 2144.
- Todd, S.W., Hoffer, R.M., Milchunas, D.G., 1998. Biomass estimation on grazed and ungrazed rangelands using spectral indices. *International Journal of Remote Sensing* 19, 427–438.
- USDI Bureau of Land Management, 1999. Sampling vegetation attributes interagency. Technical reference.
- USDI Bureau of Land Management, 1997. Idaho standards for rangeland health and guidelines for livestock grazing management.
- Vautherin, J., 2016. Photogrammetric accuracy and modeling of rolling shutter cameras. EuroCOW 2016, European Calibration Orientation Work (presentation), 10–12 February 2016, Lausanne, Switzerland.
- Veblen, K.E., Pyke, D.A., Aldridge, C.L., Casazza, M.L., Assal, T.J., Farinha, M.A., 2014. Monitoring of livestock grazing effects on bureau of land management land. *Rangeland Ecology & Management* 67, 68–77.
- Wang, H., Wang, C., Price, K.P., van der Merwe, D., An, N., 2014. Modeling Above-Ground Biomass in Tallgrass Prairie Using Ultra-High Spatial Resolution sUAS Imagery. *Photogrammetric Engineering & Remote Sensing* 80, 1151–1159.
- Washington-Allen, R.A., West, N.E., Ramsey, R.D., Efromyson, R.A., 2004. A protocol for retrospective remote sensing-based ecological monitoring of rangelands. *Rangeland Ecology & Management* 59, 19–29.
- Westoby, M.J., Brasington, J., Glasser, N.F., Hambrey, M.J., Reynolds, J.M., 2012. 'Structure-from-Motion' photogrammetry: a low-cost, effective tool for geoscience applications. *Geomorphology* 179, 300–314.
- Wheaton, J.M., Brasington, J., Darby, S.E., Sear, D.A., 2009. Accounting for uncertainty in DEMs from repeat topographic surveys: improved sediment budgets. *Earth Surface Processes and Landforms* 156, 136–156.